Practical considerations for the ion channel free-electron laser

B. Ersfeld[1], R. Bonifacio[1], S. Chen[1], M.R. Islam[1], and D.A. Jaroszynski[1]

[1] Department of Physics, Scottish Universities Physics Alliance and University of Strathclyde, Glasgow G4 0NG, United Kingdom

ABSTRACT

The ion-channel laser (ICL) has been proposed as an alternative to the free-electron laser (FEL), replacing the deflection of electrons by the periodic magnetic field of an undulator with the periodic betatron motion in an ion channel. Ion channels can be generated by passing dense energetic electron bunches or intense laser pulses through plasma. The ICL has potential to replace FELs based on magnetic undulators, leading to very compact coherent X-ray sources. In particular, coupling the ICL with a laser plasma wakefield accelerator would reduce the size of a coherent light source by several orders of magnitude. An important difference between FEL and ICL is the wavelength of transverse oscillations: In the former it is fixed by the undulator period, whereas in the latter it depends on the betatron amplitude, which therefore has to be treated as variable. Even so, the resulting equations for the ICL are formally similar to those for the FEL with space charge taken into account, so that the well-developed formalism for the FEL can be applied. The amplitude dependence leads to additional requirements compared to the FEL, *e.g.* a small spread of betatron amplitudes. We shall address these requirements and the resulting practical considerations for realizing an ICL, and give parameters for operation at UV fundamental wavelength, with harmonics extending into X-rays.

Keywords: ion channel, free-electron laser, betatron oscillations, coherent X-ray source

1. INTRODUCTION

The free-electron laser (FEL)[1,2] produces highly coherent, ultra-short duration light pulses with extremely high peak brilliance, and photon energies extending to above 10 keV. FELs are very useful for ultrafast time-resolved studies of the structure of matter but require high energy electron beams and long undulators, which makes them large and expensive. In spite of the high cost, several large national and international X-ray FELs[3] have been, or are being, built because of their potential for delivering new science and applications.

FELs are based on the collective interaction of high energy electrons that are periodically deflected by an undulator. The combined undulator and radiation fields give rise to a ponderomotive force that bunches the electrons on a wavelength scale and results in intense coherent emission. The self-amplified spontaneous emission (SASE) FEL[2] produces coherent radiation by amplifying incoherent synchrotron radiation spontaneously emitted by the initially uncorrelated electron beam.

However, magnetostatic undulators are not the only means of providing a periodic transverse force. Whittum *et al.*[4] suggested in 1990 that an ion-channel laser (ICL) could use the "betatron" motion of electrons in an ion-channel to emulate an undulator, resulting in a very compact device.

An important difference between the FEL and ICL is the spatial periodicity of the transverse oscillations. In the FEL, this is fixed by the undulator, whereas in the ICL it depends on the ion density, and both the electron energy and oscillation amplitude. Due to this latter dependence, maintaining resonance with the emitted field in an ICL requires a small amplitude spread, unless the transverse momentum is very small. Only the latter case with very small amplitudes was treated in Refs.[4–6]. However, this is constrained to very low emittances, that are very difficult to achieve in practice.

We have recently[7] investigated the more general and realistic case of high transverse momentum, which requires the betatron amplitude to be treated as variable. Assuming ultra-relativistic axial and high transverse

Further author information: (Send correspondence to B.E.)
B.E.: E-mail: bernhard.ersfeld@strath.ac.uk, Telephone: +44 141 5485750
D.A.J.: E-mail: dino@phys.strath.ac.uk, Telephone: +44 141 5483057

Relativistic Plasma Waves and Particle Beams as Coherent and Incoherent Radiation Sources
edited by Dino A. Jaroszynski, Proc. of SPIE Vol. 9509, 95090L · © 2015 SPIE
CCC code: 0277-786X/15/$18 · doi: 10.1117/12.2178989

Downloaded From: http://spiedigitallibrary.org/ on 01/15/2016 Terms of Use: http://spiedigitallibrary.org/ss/TermsOfUse.aspx

momenta, but non-relativistic transverse velocity, we have derived a set of equations for the ICL in the steady-state regime describing, on a slow timescale, the complex amplitude of the amplified wave, and the axial momenta, betatron amplitudes, and ponderomotive phases of the oscillating electrons. Space-charge effects have been included.

The study demonstrated that the form of the equations allows to apply the well-known scaling procedure for the FEL, with an analogous fundamental coupling parameter ρ [2], and presented analytical and numerical results presented showing that for small ρ the evolution of field amplitude, phase bunching, and axial momentum in the ICL is virtually identical to the FEL. We have investigated how the growth of the radiation field depends on the initial spreads of axial electron momentum and betatron amplitude and found that the admissible betatron amplitude spreads lead to a small source size for the emitted radiation, which necessitates guiding to avoid diffraction. Small overlap between the radiating electrons and the guided mode makes space-charge effects relatively much more important than in the FEL.

Here, we concentrate on the practical requirements imposed by the conditions of small energy and amplitude spreads on experimental realizations of the ICL. Small betatron amplitude spreads (compared to the mean oscillation amplitude) can be achieved by injecting the electrons off-axis and/ or under an angle, as shown schematically, for just two electrons, in Fig. 1. We show that at large values of ρ electron beams with realistic amplitude spreads and emittance can be used to drive the ICL efficiently at fundamental wavelengths down to UV, with harmonics extending into X-rays.

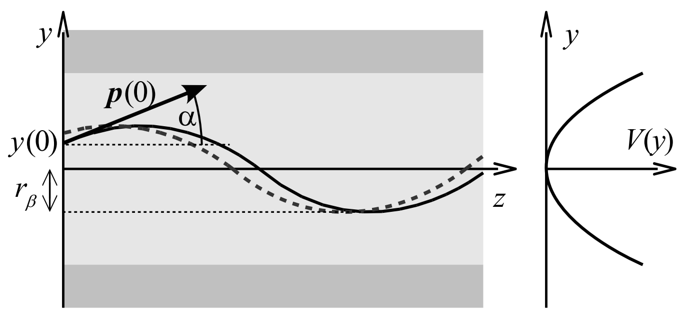

Figure 1. Schematic of electron injection into the ion channel. An offset in position ($y(0)$) and/ or momentum ($p(0)$) from the channel axis (z-axis) leads to betatron oscillations (solid trajectory) in the parabolic potential $V(y)$, with amplitude r_β. The dashed trajectory is for an electron with slightly different initial conditions, but equal r_β. An electron bunch with suitable initial distribution in phase space can have a small betatron amplitude spread.

2. ELECTRON AND FIELD DYNAMICS

In Ref.[7], we have investigated the ion-channel laser with large variable oscillation amplitude. In the following, we reproduce the assumptions underlying the model and the results to provide a basis for understanding the operating conditions for an ICL:

The potential energy of a test electron in a cylindrical plasma channel with background density n_0 along the z-axis is

$$V = m\omega_p^2 y^2/4, \quad \text{with} \quad \omega_p = [e^2 n_0/(\varepsilon_0 m)]^{1/2}$$

being the plasma frequency (where $-e$ and m are the electron charge and mass, respectively, and ε_0 is the vacuum permittivity).
The Hamiltonian for motion in the y-z-plane is

$$H = \gamma mc^2 + V, \quad \text{with} \quad \gamma = [\gamma_0^2 + (p_y + eA)^2/(mc)^2]^{1/2} \quad \text{and} \quad \gamma_0 = [1 + p_z^2/(mc)^2]^{1/2},$$

where p_y and p_z are radial and axial components, respectively, of the canonical momentum, and

$$A = a_0 mc \exp(-i\phi)/(2e) + c.c.$$

Downloaded From: http://spiedigitallibrary.org/ on 01/15/2016 Terms of Use: http://spiedigitallibrary.org/ss/TermsOfUse.aspx

is the.vector potential of a propagating wave, linearly polarized along the y-axis, with phase $\phi = \omega t - kz$, ($\omega \approx ck$), and slowly varying complex amplitude a_0.

The test electron will perform betatron oscillations

$$y(t) = r_\beta \cos(\omega_\beta t),$$

with amplitude r_β, frequency $\omega_\beta = \omega_p/(2\gamma)^{1/2}$, and associated energy

$$W_\beta = H - \gamma_0 mc^2 = m\omega_p^2 r_\beta^2/4 \approx \gamma_0 m v_y^2/2 + V \ll \gamma_0 mc^2,$$

with $v_y = (p_y + eA)/(\gamma_0 m) = -v_\beta \sin(\omega_\beta t)$, and $v_\beta = \omega_\beta r_\beta \ll c$.
The betatron energy evolves as $\dot{W}_\beta = v_y e\dot{A} - m v_y^2 \dot{\gamma}_0/2$, where the dot designates the total time derivative, $d_t = \partial_t + v_z \partial_z$, and hence the betatron amplitude, on a slow scale, as

$$\dot{r}_\beta = [ic\, \dot{a}_0 \exp(i\theta) + c.c.]/[2\omega_p (2\gamma_0)^{1/2}] - r_\beta \dot{\gamma}_0/(4\gamma_0). \tag{1}$$

The corresponding axial ponderomotive force is

$$\dot{p}_z|_{pond} = \eta_h m\omega a_0 v_\beta \exp(i\theta)/4 + c.c.,$$

where $\theta = \omega_\beta t - \phi$ is the ponderomotive phase. The factor

$$\eta_h = \mathrm{J}_0(Q_\beta) - \mathrm{J}_1(Q_\beta), \quad \text{with} \quad Q_\beta = k r_\beta v_\beta/(8c),$$

and where $\mathrm{J}_{0,1}$ are Bessel functions, accounts for the modulation of the axial velocity[8]:

$$v_z = \bar{v}_z + v_m \cos(2\omega_\beta t),$$

with $v_m = v_\beta^2/(4c)$, $\bar{v}_z = v_{0z} - v_m$, and $v_{0z} = c[1 - 1/(2\gamma_0^2)]$.

Betatron oscillations and wave are in resonance when the ponderomotive phase is stationary. At the position $z(t) = z(0) + \bar{v}_z t$ of the electron, with time-averaged velocity $\bar{v}_z$, the phase evolves as

$$\dot{\theta} = \omega_\beta - \omega(1 - \bar{v}_z/c) \approx \omega_\beta - \omega/(2\bar{\gamma}_z^2), \quad \text{with} \quad \bar{\gamma}_z = (1 - \bar{v}_z^2/c^2)^{-1/2} \approx \gamma_0/(1 + a_\beta^2/2)^{1/2};$$

the betatron parameter $a_\beta = \gamma_0 v_\beta/c$ is the normalized amplitude of transverse momentum. Resonance thus occurs for $\omega = \omega_p(2\gamma_0^3)^{1/2}/[1 + \gamma_0 \omega_p^2 r_\beta^2/(4c^2)]$. For $a_\beta \gg 1$, which for very high γ_0 is possible although $v_\beta \ll c$,

$$\dot{\theta} = \omega_p (2\gamma_0)^{-1/2} - \omega\omega_p^2 r_\beta^2/(8\gamma_0 c^2), \tag{2}$$

and the resonance condition is $\gamma_0 = \gamma_{res}$, with

$$\gamma_{res} = \omega^2 \omega_p^2 r_\beta^4/(32\, c^4). \tag{3}$$

In an electron bunch, space-charge forces[8] contribute to the slow longitudinal force; thus

$$\dot{\gamma}_{0j} = \Big[\frac{\eta_h \omega v_{\beta j}}{4c}\, a_0 - i\eta_f \frac{\omega_b^2}{\omega} \langle \exp(-i\theta)\rangle\Big] \exp(i\theta_j) + c.c., \tag{4}$$

where in the space-charge term, proportional to $\omega_b^2 = \omega_p^2\, n_b/n_0$, where n_b is the density in the bunch, the angled brackets denote an average over the electrons in a slice; $\eta_f = \min(\sigma(y)/\langle r_\beta \rangle, 1)$ accounts for the finite width $\sigma(y)$ of the electron bunch.

The radiation from these electrons contributes to the wave amplitude:

$$(\partial_t + c\partial_z) a_0 = -\eta_h \eta_m \eta_f \omega_b^2 \langle v_\beta \exp(-i\theta)\rangle/(2\omega c). \tag{5}$$

Downloaded From: http://spiedigitallibrary.org/ on 01/15/2016 Terms of Use: http://spiedigitallibrary.org/ss/TermsOfUse.aspx

Here η_h, defined above, accounts for the reduced emission at the fundamental frequency of the harmonic spectrum[8]. For a planar source, the amplitude of the ℓth harmonic evolves as

$$(\partial_t + c\partial_z)a_0^{(\ell)} \approx -\eta_m\eta_f\omega_b^2\langle v_\beta F_\ell(Q_\beta)\exp(-i\ell\theta)\rangle/(2\ell\omega c), \quad \text{with} \quad F_\ell(Q) = \mathrm{J}_{(\ell-1)/2}(\ell Q) - \mathrm{J}_{(\ell+1)/2}(\ell Q).$$

The resulting spectrum has a synchrotron-like envelope, with critical frequency $\omega_c \approx 3a_\beta^3\omega/8$. In resonance, $Q_\beta = a_\beta^2/(4+2a_\beta^2)$; $\eta_h \equiv F_1(Q_\beta) \approx 0.7$ for $a_\beta \gg 1$. η_m accounts for the spatial overlap of current density and radiation mode.

In the following, we neglect slippage between electrons and wave, as in the steady-state FEL regime[2], thus $d_t \approx \partial_t + c\partial_z$. Combining Eqs. (1) and (5) then yields $\langle\gamma_0^{-1/2}d_t(\gamma_0^{1/2}r_\beta^2)\rangle = 0$, implying that $\langle a_\beta r_\beta\rangle \propto \langle\gamma_0^{1/2}r_\beta^2\rangle$ is conserved if correlations between electron energy and ponderomotive phase can be neglected.

3. FEL SCALING

Neglecting slippage, Eqs. (1), (2), and (4), for each electron, and (5) form a closed set of equations, which are similar to the FEL equations[2]. In analogy to the FEL-parameter, we define

$$\rho = [\eta\omega_b^2R_\beta^2/(8\tilde{\gamma}_0c^2)]^{1/3} = [\eta(n_b/n_0)\tilde{v}_\beta^2/(4c^2)]^{1/3} \approx 0.13[\eta_m\eta_f(n_b/10^{18}\,\mathrm{cm}^{-3})(R_\beta/\mu\mathrm{m})^2/\tilde{\gamma}_0]^{1/3}, \tag{6}$$

where $\tilde{\gamma}_0 = \langle\gamma_0\rangle(0)$ and $R_\beta = \langle\gamma_0^{1/2}r_\beta^2\rangle^{1/2}/\tilde{\gamma}_0^{1/4}$ are the initial average energy and betatron amplitude, respectively; furthermore, $\tilde{v}_\beta = \tilde{\omega}_\beta R_\beta$, $\tilde{\omega}_\beta = \omega_p/(2\tilde{\gamma}_0)^{1/2}$, and $\eta = \eta_h^2\eta_m\eta_f$.
For typical experimental parameters, $n_b = 10^{16}...10^{20}\,\mathrm{cm}^{-3}$, $R_\beta = 1...10\,\mu\mathrm{m}$, $\tilde{\gamma}_0 = 10^2...10^3$, $\eta_m = 0.01...0.1$, and $\eta_f = 10^{-6}...0.1$, we find $\rho \approx 6\cdot10^{-6}...0.13$. Higher values of ρ could be obtained for relativistic transverse velocities, which are beyond the scope of this study.
In the following, we use $\eta_m \approx 0.01$ corresponding to propagation in a channel surrounded by underdense plasma, which will be discussed below.

We scale the vector potential amplitude

$$\bar{a}_0 = -\eta_h a_0/(\rho^2\tilde{a}_\beta), \quad \text{with} \quad \tilde{a}_\beta = \tilde{\gamma}_0\tilde{v}_\beta/c,$$

and define relative deviations $q_j = \gamma_{0,j}/\tilde{\gamma}_0 - 1$ of the energies $\gamma_{0,j}$, and $s_j = r_{\beta,j}(\gamma_{0,j}/\tilde{\gamma}_0)^{1/4}/R_\beta - 1$ of the betatron amplitudes $r_{\beta,j}$, of individual electrons from the initial averages, and the average detuning from resonance $\delta \equiv (\tilde{\gamma}_0/\left.\gamma_{res}\right|_{r_\beta=R_\beta})^{1/2} - 1$. With this, the evolution equations become

$$\begin{aligned}
\bar{a}_0' &= (1+\delta)\langle(1+s)\exp(-i\theta)/(1+q)^{3/4}\rangle, && (7)\\
\theta_j' &= \bar{P}_j \equiv \rho^{-1}\{(1+q_j)^{-1/2} - (1+s_j)^2/[(1+\delta)(1+q_j)^{3/2}]\}, && (8)\\
q_j' &= -\rho\bar{a}_0(1+s_j)\exp(i\theta_j)/[(1+\delta)(1+q_j)^{3/4}] - 2i\rho^2(1+\delta)\langle\exp(-i\theta)\rangle\exp(i\theta_j)/(\eta_h^2\eta_m) + c.c., && (9)\\
s_j' &= -i[\rho^2/(4\eta_h)]\bar{a}_0'[\exp(i\theta_j)/(1+q_j)^{1/4}] + c.c., && (10)
\end{aligned}$$

where the prime denotes the derivative with respect to the scaled time

$$\tau = \rho\tilde{\omega}_\beta t.$$

Eqs. (9) and (10) suggest scaling

$$\bar{q}_j = q_j/\rho, \quad \bar{s}_j = 2\eta_h s_j/\rho^2, \quad \text{and} \quad \bar{\delta} = \delta/\rho.$$

If q_j, s_j, and δ are small compared to unity, Eqs. (7) to (10) may be linearised and, using $\bar{P}_j \approx \bar{q}_j - \rho\bar{s}_j/\eta_h + \bar{\delta}$, the last two merged to obtain

$$\begin{aligned}
\bar{a}_0' &= \langle\exp(-i\theta)\rangle, && (11)\\
\theta_j' &= \bar{P}_j, && (12)\\
\bar{P}_j' &= -[\bar{a}_0 + i\tilde{\rho}\langle\exp(-i\theta)\rangle]\exp(i\theta_j) + c.c., && (13)
\end{aligned}$$

Downloaded From: http://spiedigitallibrary.org/ on 01/15/2016 Terms of Use: http://spiedigitallibrary.org/ss/TermsOfUse.aspx

with

$$\tilde{\rho} = \rho(4/\eta_m - \eta_h)/(2\eta_h^2).$$

Except for this coefficient (rather than ρ), these eqs. are nearly identical to those of the FEL with space-charge[8]. However, due to the small value of η_m, space-charge effects are relatively enhanced.

For small signal, assuming $\bar{a}_0 \propto \exp(i[\kappa - \bar{\delta}]\tau)$ results in the secular equation

$$\kappa^3 - \kappa^2\bar{\delta} - \kappa\tilde{\rho} + 1 + \tilde{\rho}\bar{\delta} = 0,$$

which is similar to that for the FEL[2]. For $\bar{\delta}$ below a threshold value, there is an unstable solution with amplitude growing exponentially at a rate $\Gamma = \rho\,\tilde{\omega}_\beta|\mathrm{Im}(\kappa)|$, which gives the gain of the ICL. For small $\bar{\delta}$ and $\tilde{\rho}$,

$$\bar{\Gamma} = \Gamma/(\rho\,\tilde{\omega}_\beta) \approx \sqrt{3}[1 - \tilde{\rho}/3 - (\bar{\delta}^2 - 2\tilde{\rho}\bar{\delta})/9]/2.$$

4. NUMERICAL RESULTS

We have numerically solved the set of Eqs. (7) to (10) for different values of ρ and δ, with small initial field, $|\bar{a}_0|(0) = 10^{-3}$, and vanishing initial bunching $b \equiv \langle(1+s)\exp(-i\theta)/(1+q)^{3/4}\rangle = 0$ (thus $\bar{a}_0'(0) = 0$). We varied the initial spreads of momenta, $\sigma(\bar{q}(0))$, and of betatron amplitudes, $\sigma(\bar{s}(0))$ (where $\sigma(f) = (\langle f^2\rangle - \langle f\rangle^2)^{1/2}$) to explore their effect on the interaction and determine the threshold conditions for a realizable ICL.

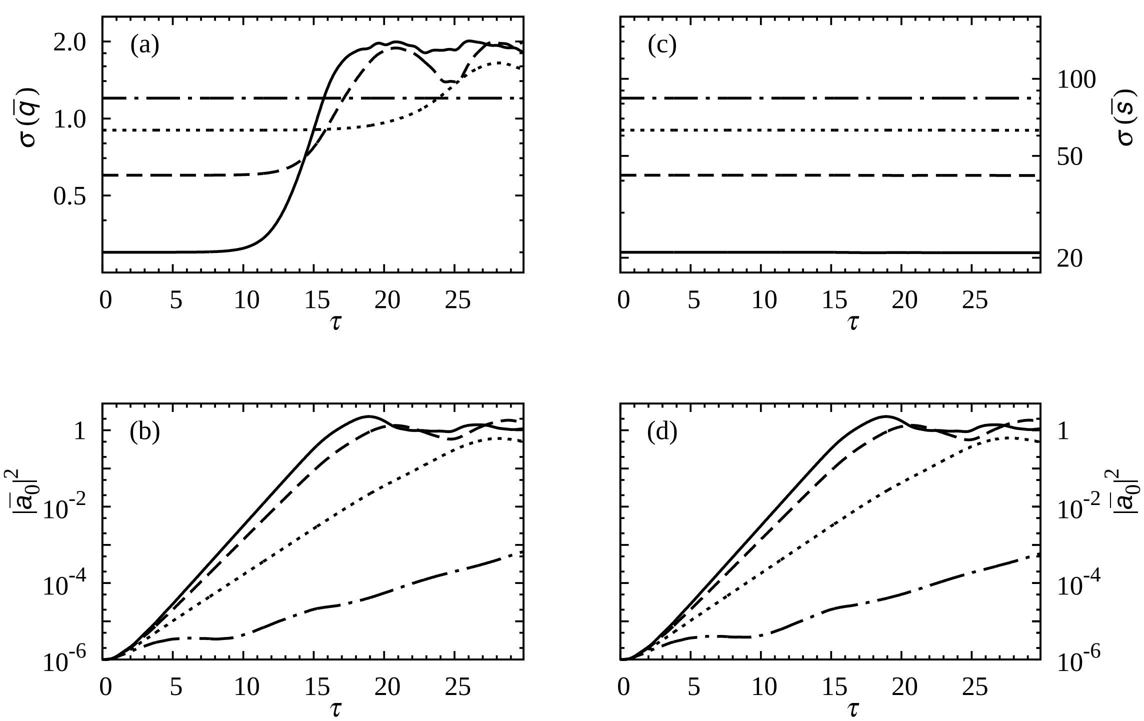

Figure 2. Evolution of spreads of momenta, $\sigma(\bar{q})$, and amplitudes, $\sigma(\bar{s})$, and corresponding field intensity $|\bar{a}_0|^2$, for $\rho = 0.01$ and varying initial conditions: (a) $\sigma(\bar{q})$ and (b) $|\bar{a}_0|^2$ for $\sigma(\bar{s}(0)) = 21$ and $\sigma(\bar{q}(0)) = 0.3$ (solid), $\sigma(\bar{q}(0)) = 0.6$ (dashed), $\sigma(\bar{q}(0)) = 0.9$ (dotted), and $\sigma(\bar{q}(0)) = 1.2$ (dot-dashed); (c) $\sigma(\bar{s})$ and (d) $|\bar{a}_0|^2$ for $\sigma(\bar{q}(0)) = 0.3$ and $\sigma(\bar{s}(0)) = 21$ (solid), $\sigma(\bar{s}(0)) = 42$ (dashed), $\sigma(\bar{s}(0)) = 63$ (dotted), and $\sigma(\bar{s}(0)) = 84$ (dot-dashed).

Figure 2 shows the spreads of momentum $\sigma(\bar{q})$, and betatron amplitude $\sigma(\bar{s})$ as functions of τ for varying initial values, together with the corresponding field intensities, for $\rho = 0.01$ and $\bar{\delta} = 2.0$, which is optimized for fastest growth. For small initial spreads, the evolution of intensity $|\bar{a}_0|^2$, bunching $|b|$, and average $|\langle\bar{q}\rangle|$ and spread $\sigma(\bar{q})$ of the momentum deviations is similar to the conventional FEL, with stages of lethargy, exponential

Downloaded From: http://spiedigitallibrary.org/ on 01/15/2016 Terms of Use: http://spiedigitallibrary.org/ss/TermsOfUse.aspx

growth, and saturation, where each of the scaled variables is of order unity and oscillates quasi-periodically[9]. If $\sigma(\bar{q})$ initially is close to its saturation value, ~ 2.0, it remains approximately constant, and the growth of the field is suppressed. Interestingly, the amplitude spread $\sigma(\bar{s})$, which does not play a role in the FEL but affects the resonance in the ICL, evolves in an analogous way to $\sigma(\bar{q})$. However, the threshold for $\sigma(\bar{s}(0))$ to suppress the growth of $|\bar{a}_0|^2$ is $\sim 0.7/\rho$; the contribution from $\sigma(\bar{s})$ to the relevant spread $\sigma(\bar{P})$ is scaled with ρ/η_h, *cf.* Eq. (12).

Varying ρ from 0 to 0.05, while maintaining optimized detuning, space-charge effects increase the scaled saturation intensity by about one third, and reduce the scaled gain coefficient by one half; for the unscaled quantities, these reductions are more than outweighed by their respective scaling, $a_0 = -\rho^2\tilde{a}_\beta\bar{a}_0$ and $\Gamma = \rho\,\tilde{\omega}_\beta\bar{\Gamma}$. The linearization yielding Eqs. (11) to (13) is valid for $\rho < 0.003$. Figure 3 shows the dependence of the growth

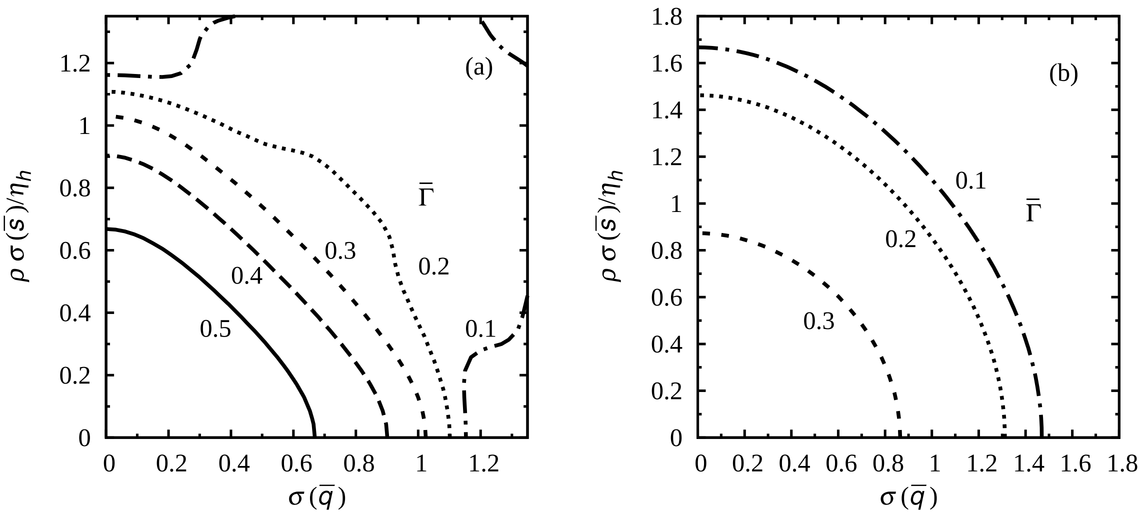

Figure 3. Contours of growth rate $\bar{\Gamma} = d\ln|\bar{a}_0|/d\tau$ for varying $\sigma(\bar{q}(0))$, and $\sigma(\bar{s}(0))$, for (a) $\rho = 0.005$, $\bar{\delta} = 1.5$, and (b) $\rho = 0.05$, $\bar{\delta} = 5.5$.

rate on initial momentum and amplitude spreads. These plots (and similar ones for the saturation amplitude) yield an approximate condition for amplification in the ICL:

$$[\sigma(\gamma_0(0))/\tilde{\gamma}_0]^2 + [\sigma(r_\beta(0))/R_\beta]^2 \le (1+10\rho)^2\rho^2, \tag{14}$$

i.e. the relative spread, between different electrons, in the variable $\bar{P}$, Eq. (8), must be less than $\sim \rho$. These admissible spreads imply optimum detuning δ. The condition $\Delta\gamma_z/\gamma_z < \rho$ in Ref.[10], referring to variations of the "axial energy" within a cycle, does not apply, since these are taken into account by the emission efficiency η_h for the fundamental frequency of the harmonic spectrum.

The dependence on the relative amplitude spread in condition (14) suggests scaling the filling factor with the FEL-parameter: $\eta_f = \rho\bar{\eta}_f$, with $\bar{\eta}_f \approx 0.5$, say. This results in a new scaling for ρ:

$$\rho = [\eta_h^2\eta_m\bar{\eta}_f\omega_b^2 R_\beta^2/(8\tilde{\gamma}_0 c^2)]^{1/2} \;\approx\; 3.3\cdot 10^{-3}[(n_b/10^{18}\,\mathrm{cm}^{-3})/\tilde{\gamma}_0]^{1/2}(R_\beta/\mu\mathrm{m}). \tag{15}$$

For the parameters given after Eq. (6), $\rho \approx 10^{-5}...0.03$.

5. PRACTICAL CONSIDERATIONS

Whittum's original proposal[4] for the ICL would be very difficult to realize experimentally, at least for high $\tilde{\gamma}_0$, due to the restriction to very small transverse momenta, $a_\beta \ll 1$, which would also lead to very low gain and low efficiency and thus unfeasibly long devices. However, our study shows that large transverse momenta can realistically be used, by explicitly taking into account the effect of the betatron amplitude on the resonance,

Downloaded From: http://spiedigitallibrary.org/ on 01/15/2016 Terms of Use: http://spiedigitallibrary.org/ss/TermsOfUse.aspx

which allows the coupled radiation-matter equations to be cast in a form similar to that of the conventional FEL.

Experimentally, an ion channel can be realized by focusing a laser pulse with relativistic amplitude $E_L > m\omega_L c/e$ (where ω_L is the laser frequency) into plasma. Its ponderomotive force displaces the electrons from its path and a "bubble" structure is formed, which provides the required transverse field in addition to a longitudinal wakefield[11]. To minimize the variation of $\tilde{\gamma}_0$, the electron bunch should be close to dephasing, at the centre of the "bubble"; as their velocities are different this limits the useful propagation length.

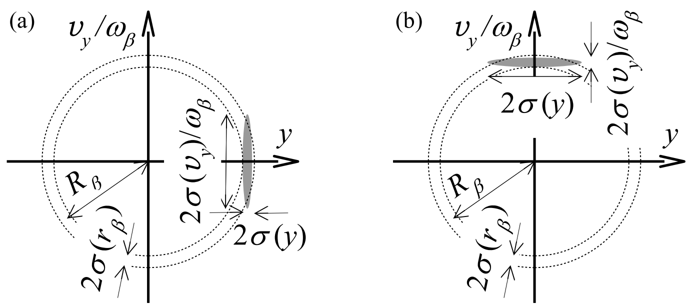

Figure 4. Schematic of initial phase-space distributions of electron bunches injected off-axis (a) and under an angle (b), respectively, with different widths $\sigma(y)$ and velocity spreads $\sigma(v_y)$, but resulting in equal betatron amplitude R_β and spread $\sigma(r_\beta) \ll R_\beta$.

Figure 4 shows possible initial phase-space distributions resulting in low amplitude spread.

Small $\sigma(r_\beta)/R_\beta$, $\sim 0.7\rho$, can be achieved by injecting electrons either off-axis at a distance R_β, with width and range of betatron phases

$$\sigma(y) \approx 0.5\rho R_\beta \quad \text{and} \quad \sigma(\varphi_\beta) \approx \sigma(v_y)/\tilde{v}_\beta \leq 0.8\sqrt{\rho},$$

respectively, or at an angle $\arctan(\tilde{v}_\beta/c)$, with

$$\sigma(v_y) \approx 0.5\rho\tilde{v}_\beta \quad \text{and} \quad \sigma(y) \approx 0.8\sqrt{\rho}R_\beta.$$

A possible way to offset an electron bunch trapped in the "bubble" from the axis would be to perturb the propagation direction of the laser and thus of the "bubble"[12].

The normalized emittance,

$$\epsilon_{yn} \approx \pi\tilde{\gamma}_0\sigma(y)\sigma(v_y)/c \leq 0.4\pi\rho^{3/2}\tilde{a}_\beta R_\beta,$$

sets a lower limit for the emitted fundamental wavelength: Using Eqs. (3) and (15), the latter is given by

$$\lambda = \pi\tilde{\omega}_\beta R_\beta^2/(2c) \geq \epsilon_{yn}/(0.8\rho^{3/2}\tilde{\gamma}_0) = 6.6\cdot 10^3\epsilon_{yn}/[(n_b/10^{18}\,\mathrm{cm}^{-3})^{3/4}(R_\beta/\mu\mathrm{m})^{3/2}\tilde{\gamma}_0^{1/4}].$$

To avoid emittance growth in the x-direction, perpendicular to the polarization, the bunch should be matched to the focusing potential; for $\epsilon_{xn} = \epsilon_{yn}$ this results in a width $\sigma(x) \leq 0.6\rho^{3/4}R_\beta$. The source size is thus $\pi\sigma(x)R_\beta/4 \leq 0.5\rho^{3/4}R_\beta^2$, and the Rayleigh length $0.5\rho^{3/4}R_\beta^2/\lambda = 0.05\rho^{3/4}\lambda_\beta$. This is shorter than the gain length, $l_g = \lambda_\beta/(\sqrt{3}\pi\rho)$ by a factor of $\sim 0.3\rho^{7/4}$, making some form of guiding necessary. Optical guiding is naturally provided by the plasma channel, since the refractive index in the channel (≈ 1) is higher than in the surrounding plasma ($\sqrt{1-\omega_p^2/\omega^2}$). An analysis similar to Ref.[13] shows that the plasma channel can guide high-frequency modes if its radius exceeds c/ω_p. For $\omega \gg \omega_p$, the overlap factor of an electron bunch oscillating inside the channel, with amplitude matched to the channel radius, with the lowest order mode is $\eta_m \approx 0.01$.

Electron bunches can be accelerated in laser wakefields to $\tilde{\gamma}_0 = 200 - 300$ with relative energy spread as small as $\sigma(\gamma_0(0))/\tilde{\gamma}_0 \sim 0.01$ [14], and normalized emittance $\epsilon_{yn} \sim 10^{-6}\,\pi\,\mathrm{m}$[15]. This emittance together with

Downloaded From: http://spiedigitallibrary.org/ on 01/15/2016 Terms of Use: http://spiedigitallibrary.org/ss/TermsOfUse.aspx

$n_b = 10^{20}\,\mathrm{cm}^{-3}$, $R_\beta = 10\,\mu$m, and $\tilde{\gamma}_0 = 300$, thus $\rho = 0.02$, yields $\lambda \geq 5\,\mu$m; for the shortest wavelength, $\tilde{\omega}_\beta = 10^{13}\,\mathrm{s}^{-1}$, $\omega_p = 2.4 \cdot 10^{14}\,\mathrm{s}^{-1}$, $n_0 = 1.8 \cdot 10^{19}\,\mathrm{cm}^{-3}$, $\tilde{v}_\beta = 10^8\,\mathrm{ms}^{-1} = 0.33c$, $\tilde{a}_\beta = 100$, and gain length $l_g = 1.7\,\mathrm{mm}$.
The critical harmonic number of the synchrotron-like spectrum is $h_c = 3a_\beta^3/8 = 3.8 \cdot 10^3$, resulting in a critical wavelength $\lambda_c = 1.3 \cdot 10^{-11}\,\mathrm{m}$. These latter values are for guidance only, as the high oscillation amplitude, larger than the bunch width, leads to a modified emission spectrum.
Improving the emittance to $\epsilon_{yn} \sim 4 \cdot 10^{-8}\,\pi\,\mathrm{m}$, as proposed in Ref. [16], allows $\lambda \geq 2 \cdot 10^{-7}\,\mathrm{m}$; in this case, $\tilde{\omega}_\beta = 4 \cdot 10^{11}\,\mathrm{s}^{-1}$, $\omega_p = 9.6 \cdot 10^{12}\,\mathrm{s}^{-1}$, $n_0 = 2.7 \cdot 10^{16}\,\mathrm{cm}^{-3}$, $\tilde{v}_\beta = 4 \cdot 10^6\,\mathrm{ms}^{-1} = 0.013c$, $\tilde{a}_\beta = 4$, $l_g = 4.5\,\mathrm{cm}$, $h_c = 24$, and $\lambda_c = 8.3 \cdot 10^{-9}\,\mathrm{m}$.
The current in these cases is $I \approx 600$A, and the efficiency of converting kinetic electron energy into radiated energy, $\rho|\bar{a}_0^2| \approx 2\%$ at saturation, giving a peak power, at the fundamental wavelength, of 2 GW and respective photon rates of $5 \cdot 10^{28}\,\mathrm{s}^{-1}$ and $2 \cdot 10^{27}\,\mathrm{s}^{-1}$.
Increasing n_b to $1.5 \cdot 10^{20}\,\mathrm{cm}^{-3}$ and R_β to $15\,\mu$m, with $\tilde{\gamma}_0 = 200$, results in $\rho = 0.049$. For emittance $\epsilon_{xn} = \epsilon_{yn} = 10^{-6}\,\pi\,\mathrm{m}$ and $\omega_p = 3.4 \cdot 10^{13}\,\mathrm{s}^{-1}$, the fundamental wavelength is $\lambda = 2\,\mu$m and the gain length 4 mm. In this case, $\tilde{a}_\beta = 17$ and $\lambda_c = 1.1 \cdot 10^{-9}\,\mathrm{m}$; the current is 10 kA, the peak power, emitted at λ, 50 GW, and the photon rate $5 \cdot 10^{29}\,\mathrm{s}^{-1}$.

A potential alternative to the essentially planar electron motion described so far is a spiralling trajectory initiated by an injection offset in one direction, but with a momentum component perpendicular to this and the channel axis. In this case, parts (a) and (b) of Fig. 4 correspond to the initial distributions in y-v_y- and x-v_x-phase space, respectively. If the betatron amplitudes in both directions are equal, the electron bunch can interact with a circularly polarized wave. Due to the constant magnitude of the transverse momentum in this case, coupling at the fundamental frequency is improved ($\eta_h = 1$). While this increases the FEL-parameter and reduces the fundamental wavelength by factors of ~ 1.4 and ~ 0.6, respectively, it also makes the synchrotron-like spectrum disappear.

6. CONCLUSIONS

Building on our recent study[7] of the ion-channel laser, where we have extended the formalism for the conventional FEL to allow for variable betatron amplitudes and shown the similar behaviour of both devices, we have here discussed possible configurations and parameters for realizing an ICL in an experiment. In addition to the requirement of small engine spread known from the FEL, in the ICL the relative amplitude spread must also be less than the analogous FEL parameter ρ. This can be achieved by using oscillation amplitudes exceeding the transverse beam size. Realistic values of ρ, up to 0.03, permit operating an ICL down to UV fundamental wavelengths, with harmonics potentially extending to X-rays.

ACKNOWLEDGMENTS

We acknowledge fruitful discussions with G.R.M. Robb and B.W.J. McNeil and support by the Engineering and Physical Sciences Research Council, United Kingdom, the Extreme Light Infrastructure Project, and the European Comission FP7 projects Laserlab-Europe (Grant 284464) and EuCARD-2 (Grant 312453).

REFERENCES

1. J. Madey, "Stimulated emission of bremsstrahlung in a periodic magnetic field," *Journ. Appl. Phys.* **42**, p. 1906, 1971.
2. R. Bonifacio, C. Pellegrini, and L. Narducci, "Collective instabilities and high-gain regime in a free electron laser," *Opt. Comm.* **50**, p. 373, 1984.
3. B. McNeil and N. Thompson, "X-ray free-electron lasers," *Nature Photon.* **4**, p. 814, 2010.
4. D. Whittum, A. Sessler, and J. Dawson, "Ion-channel laser," *Phys. Rev. Lett.* **64**, p. 2511, 1990.
5. K. Chen, T. Katsouleas, and J. Dawson, "On the amplification mechanism of the ion-channel laser," *IEEE Transactions on Plasma Science* **18**, p. 837, 1990.
6. K. Chen, J. Dawson, A. Lin, and T. Katsouleas, "Unified theory and comparative study of cyclotron masers, ion-channel lasers, and free electron lasers," *Phys. Fluids B* **3**, p. 1270, 1991.

Downloaded From: http://spiedigitallibrary.org/ on 01/15/2016 Terms of Use: http://spiedigitallibrary.org/ss/TermsOfUse.aspx

7. B. Ersfeld, R. Bonifacio, S. Chen, M. Islam, P. Smorenburg, and D. Jaroszynski, “The ion channel free-electron laser with varying betatron amplitude,” *New. J. Phys.* **16**, p. 093025, 2014.
8. J. Murphy, C. Pellegrini, and R. Bonifacio, “Collective instability of a free electron laser including space charge and harmonics,” *Opt. Comm.* **53**, p. 197, 1985.
9. D. Jaroszynski, R. Bakker, A. van der Meer, D. Oepts, and P. van Amersfoort, “Experimental observation of limit-cycle oscillations in a short-pulse free-electron laser,” *Phys. Rev. Lett.* **70**, p. 3412, 1993.
10. E. Esarey, B. Shadwick, P. Catravas, and W. Leemans, “Synchrotron radiation from electron beams in plasma-focusing channels,” *Phys. Rev. E* **65**, p. 056505, 2002.
11. A. Pukhov, S. K. S. Gordienko, and I. Kostyukov, “The bubble regime of laser-plasma acceleration: Monoenergetic electrons and the scalability,” *Plasma Phys. Control. Fusion* **46 B**, p. 179, 2004.
12. A. Reitsma and D. Jaroszynski, “Propagation of a weakly nonlinear laser pulse in a curved plasma channel,” *Phys. Plasmas* **14**, p. 053104, 2007.
13. E. Snitzer, “Cylindrical dielectric waveguide modes,” *J. Opt. Soc. Am.* **51**, p. 491, 1961.
14. S. Wiggins, R. Issac, G. Welsh, E. Brunetti, R. Shanks, M. Anania, S. Cipiccia, G. Manahan, C. Aniculaesei, B. Ersfeld, M. Islam, R. Burgess, G. Vieux, W. Gillespie, A. MacLeod, S. van der Geer, M. de Loos, and D. Jaroszynski, “High quality electron beams from a laser wakefield accelerator,” *Plasma Phys. Control. Fusion* **52**, p. 124032, 2010.
15. E. Brunetti, R. Shanks, G. Manahan, M. Islam, B. Ersfeld, M. Anania, S. Cipiccia, R. Issac, G. Raj, G. Vieux, G. Welsh, S. Wiggins, and D. Jaroszynski, “Low emittance, high brilliance relativistic electron beams from a laser-plasma accelerator,” *Phys. Rev. Lett.* **105**, p. 215007, 2010.
16. B. Hidding, G. Pretzler, J. Rosenzweig, T. Königstein, D. Schiller, and D. Bruhwiler, “Ultracold electron bunch generation via plasma photocathode emission and acceleration in a beam-driven plasma blowout,” *Phys. Rev. Lett.* **108**, p. 035001, 2012.

Downloaded From: http://spiedigitallibrary.org/ on 01/15/2016 Terms of Use: http://spiedigitallibrary.org/ss/TermsOfUse.aspx